

Cold Cracking and Segregation in Multi-Pass Welds of a Quenched and Tempered Steel

G. L. F. Powell

Adelaide University, Adelaide,
South Australia 5005

V. M. Linton

Adelaide University, Adelaide,
South Australia 5005

I. H. Brown

Adelaide University, Adelaide,
South Australia 5005

J. L. Davidson

Maritime Platforms Division
Defence Science and Technology Organisation
Victoria 3207

Abstract

When assessing the susceptibility of a steel weldment to hydrogen assisted cold cracking (HACC) consideration is usually given to the presence of the following factors – stress (both residual and applied), hydrogen and a susceptible microstructure. Segregation is generally not taken into account. This paper examines the correlation between cold cracking and segregation in “fish eyes” and in banding. In the fish eyes all four solute alloying elements present in the weld metal segregated intercellular-dendritically whilst unexpectedly only manganese segregated in the banded region. Cracking was found to be associated with both forms of segregation.

Introduction

Hydrogen assisted cold cracking in the welds of carbon manganese and low alloy steels has been studied extensively (1,2). In addition to stress, hydrogen and a susceptible microstructure are considered to be important factors when assessing the probability of HACC occurring. The usual method used to predict the susceptibility of the weld microstructure to HACC is to calculate the carbon equivalent based on the nominal composition of the weld metal. However, predictions based on this methodology may well be misleading as it has long been recognised that segregation of alloying elements occurs during the solidification of welds (3,4). In low alloy steels segregation may be either on a macroscopic scale e.g. solute banding, which occurs at right angles to the solidification growth direction (5) or on a microscopic scale e.g. intercellular-dendritic, which occurs parallel to the solidification growth direction (6). Low alloy steels solidify as delta ferrite (7) that subsequently transforms to austenite and then to alpha ferrite. The segregation that occurs during the solidification of the liquid to delta ferrite persists to room temperature regardless of the solid state allotropic changes occurring with decreasing temperature. The intercellular-dendritic segregation is usually not detected when these steels are etched in Nital and examined with the aid of a reflected light microscope but may be detected with

electron optical techniques if there is a change in microstructure to bainite/martensite. The use of Le Pera's reagent as an etchant (8) does show the presence of segregation but does not indicate which elements have segregated or by how much. In a previous study (5) the use of this etchant to reveal the presence of intercellular-dendritic segregation in a low alloy steel weld containing manganese and nickel was reported. As part of that study the concentration of these elements was measured using a scanning electron microscope with X-ray analytical facilities and found to be approximately 1.4 times that of the nominal weld metal composition. In a further study (6) Le Pera's reagent was also used to reveal the solute enriched intercellular-dendritic regions of a similarly alloyed steel weld. The hardness of these regions was found to be 100 Hardness Vickers higher than the weld metal matrix due to the presence of bainite/martensite.

There appears to be little reported in the literature on the role of segregation in fish eye formation. A fish eye is defined as “a discontinuity found on the fracture surface of a steel weld and consists of a small pore or inclusion surrounded by an approximately round bright area” (9). The association of fish eyes and hydrogen assisted cold cracking has been noted in the literature for many years and, inter alia, fish eyes were thought to have occurred during fracture (10). Examination of fish eyes in a field emission scanning electron microscope (FESEM) has shown that the fracture through the fish eye is partly intergranular and partly transgranular cleavage (11). This fracture mechanism is commonly associated with hydrogen embrittlement (11).

This manuscript examines the fracture within fish eyes with respect to segregation. Also reported is banding segregation of an unexpected composition containing cracking.

Experimental

Two compact tensile test specimens for fracture toughness testing were machined from multi-submerged arc welds in quenched and tempered HSLA steel plate after the welds had been radiographed. Specimens 50mm x 50mm x 10mm thick

were notched to a depth of 18mm and pre-cracked in fatigue prior to tensile testing. The composition of the weld metal is shown in Table 1 and the welding conditions in Table 2.

Element	Weight percent
Carbon	0.076
Manganese	1.37
Silicon	0.381
Nickel	2.43
Chromium	0.34
Phosphorus	0.013
Sulphur	0.005
Molybdenum	0.5

Table 1. Weld metal composition

Process	Submerged arc
Wire diameter	4mm
Polarity	Positive
Flux	OP121TT
Number of passes	63
Filler metal	LTEC120
AWS classification	SPA5 23EM4 MIL-120-1, MIL-E-23765/2B
Unit pass preheat temperature	Less than or equal to 40°C
Arc voltage	30V
Arc current	400A
Travel speed	9.3mm/sec

Table 2. Welding conditions

The fracture surfaces of the specimens were examined using stereo light microscopy and the FESEM. A section parallel to the fracture surface and 5mm below the surface was metallographically polished and examined using reflected light microscopy, FESEM and electron probe micro-analysis (EPMA) in both the unetched and etched (2% Nital) conditions. A Cameca SX51 Microprobe with 4 multicrystal Wavelength Dispersive Spectrometers (WDS), standardised using standards of pure elements, was used for the quantitative line scans of the polished and unetched surface of the section taken parallel to the fracture surface. The line scans of the surface were taken in a direction perpendicular to the crack tips.

Results

Radiography A radiograph of the welds was taken prior to mechanical testing. The presence of fish eyes was apparent.

Examination of fracture surfaces Two mating fracture surfaces as viewed through the stereo light microscope are shown in Figure 1. The shiny region of the machined notch, several fish eyes and three distinct fracture zones are present. The boundaries between the fracture zones are indicated by short arrows in Figure 1.

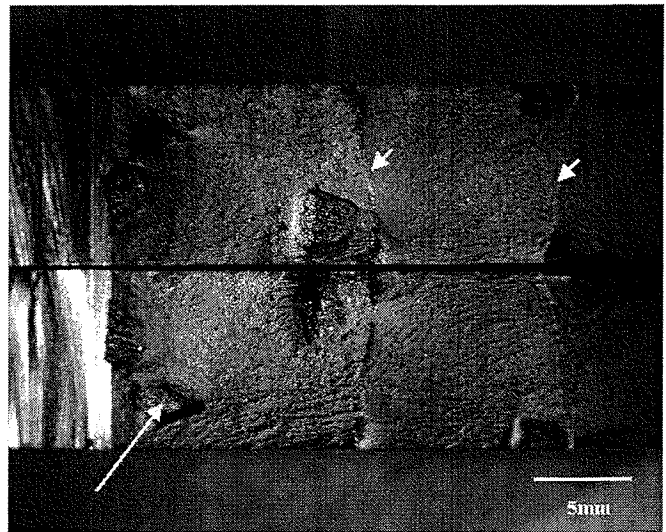


Figure 1. Optical macrograph of the mating fracture surfaces of the Compact Tension Specimen after mechanical testing. The long arrow indicates the fish eye and the shorter arrows the curved delineation between the fracture regions.

The fracture surfaces were examined in the FESEM with particular attention to the regions identified using the stereo microscope as containing fish eyes. Figure 2 - 4 are micrographs taken with the FESEM of the fish eye identified by the long arrow in Figure 1. The overall appearance of the fish eye is shown in Figure 2 with Figure 3 showing the initiation site of the fish eye. This region is characterised by a smooth, clean surface indicating the presence of a gas pore formed by a reducing gas. The fracture surface and cracking within the fish eye are shown in Figure 4. Note the cracks are both in the plane of the image and at a high angle to the plane of the image. The latter cracks are approximately 50µm apart.

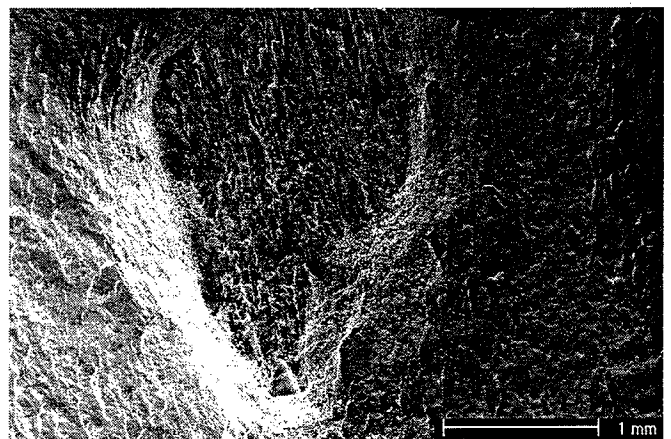


Figure 2. FESEM of the fish eye arrowed in Fig. 2. The smooth initiation region containing the gas pore and the directional cleavage type fracture within the fish eye can be seen.

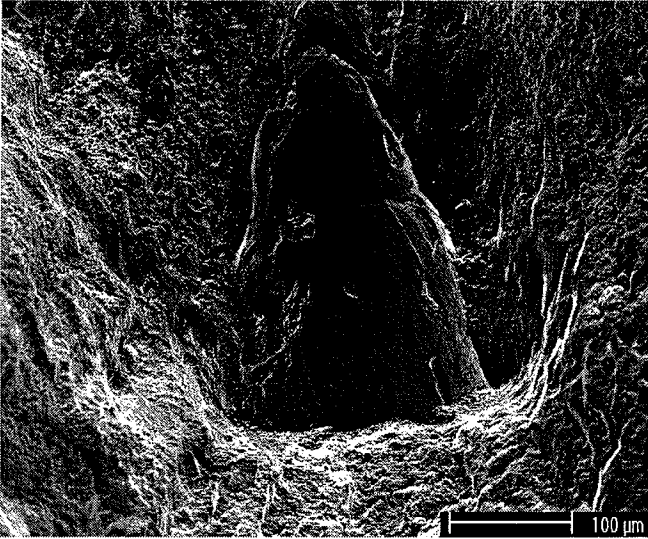


Figure 3. FESEM image of the gas pore shown in Fig. 2 at higher magnification.

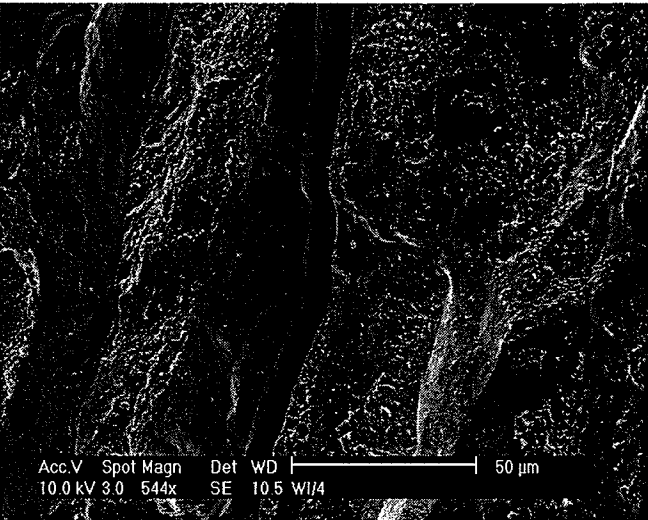


Figure 4. FESEM image of the directional cleavage mode of cracking within the fish eye

Examination of parallel section Fish eyes were visible on the cut surface after metallographic preparation. An optical micrograph of the unetched metallographically prepared section 5mm below and parallel to the fracture surface is shown in Figure 5. This figure shows the nature of the cracking through a fish eye in a plane parallel to the fracture surface.

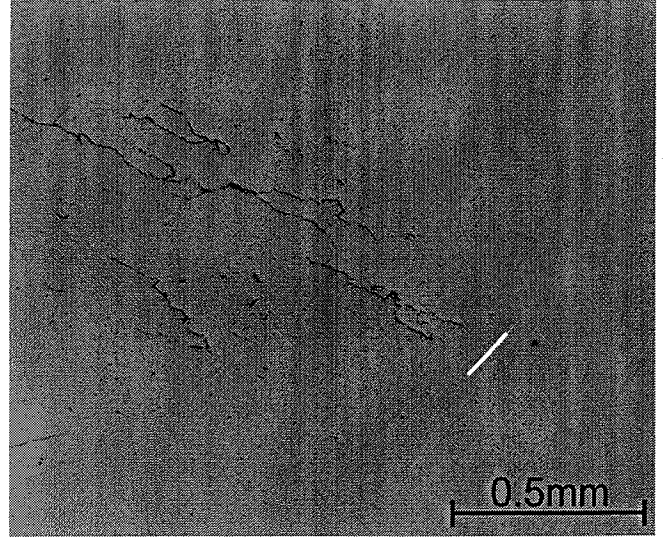


Figure 5. Optical micrograph of the cracking through a fish eye. The fish eye was approximately 5mm below the fracture surface. The white marker indicates the position of the X-ray line scan (Figure 11). Unetched.

On the same surface there was a long curved crack. This was unrelated to the cracking associated with the fish eye. An optical micrograph of the crack is shown in Figure 6.

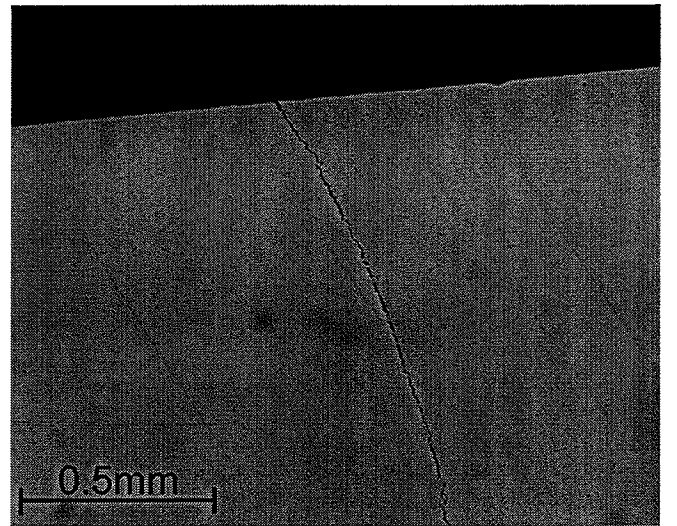


Figure 6. Optical micrograph of a long curved crack on the same surface as seen in Figure 5. Unetched.

After etching in Nital it can be seen (Figure 7) that the cracking has occurred in a banded region. The dark etched banding is more obvious in Figure 8 taken at a higher magnification near the tip of the crack.

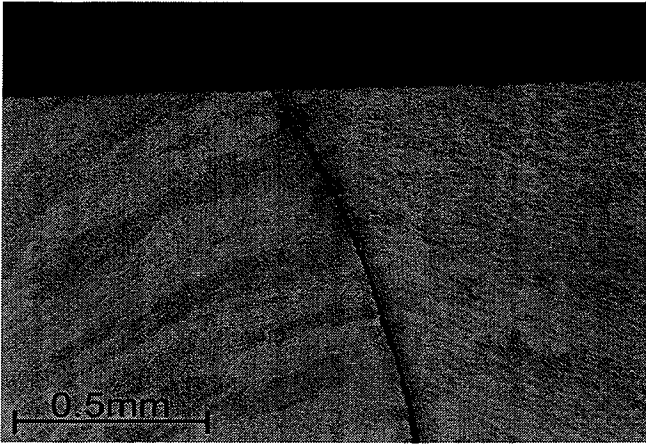


Figure 7. Same area as Figure 6 after etching in 2% Nital.

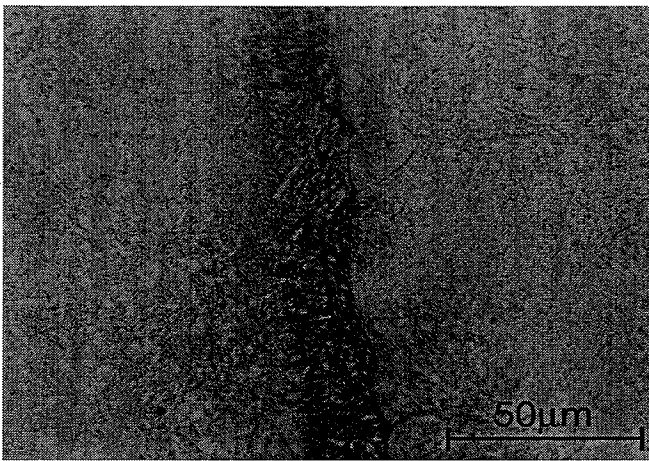


Figure 8 End of the crack shown in Figures 6 and 7. The crack is contained within a dark etching band. Etchant 2% Nital

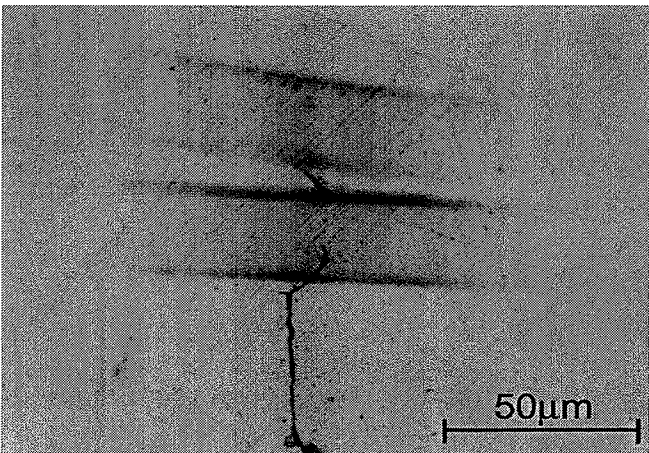


Figure 9. Repolished surface of the region shown in Figure 8. The regions between the two sets of dark parallel lines indicate the positions of the X-ray line scans.

The positions of the line scans can be identified by the dark lines on the surface. Quantitative data for one of the line scans is presented graphically in Figure 10, with the results from the other line scan being identical.

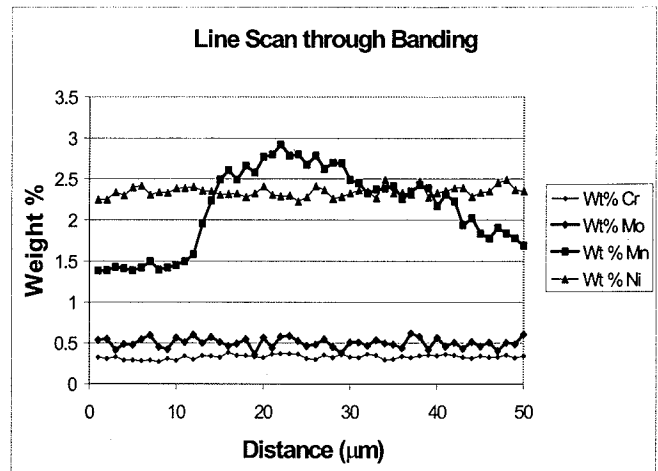


Figure 10. X-ray line scans through the banded region indicated in Figure 9. Note that manganese is the only element to have increased in concentration.

Figure 11 is a graphical representation of the line scan ahead of the crack tip shown in Figure 5. The white line indicates the position of the line scan.

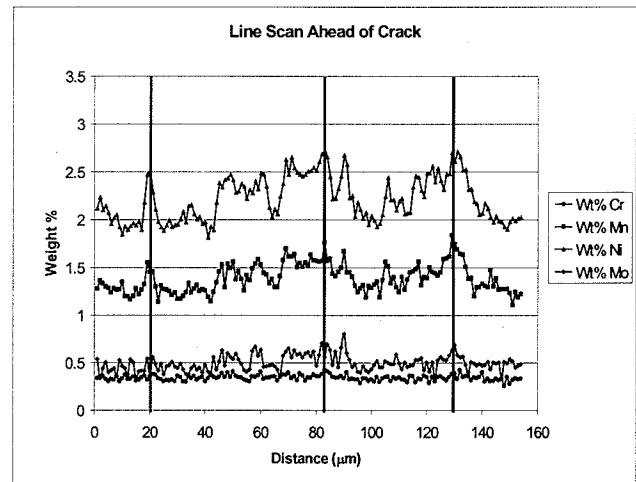


Figure 11. X-ray line scans along the line indicated in Figure 6. Vertical lines have been added through the peaks.

It should be noted that the X-ray peaks for each element are coincident, and the major peaks as indicated by the vertical lines on Figure 11, occur at intervals of approximately 50µ.m. The ratio of the peak to background for each of the elements at the positions indicated by the vertical lines is approximately 1.4.

Discussion

Fish eyes Fish eyes, often associated with HACC, were identified on the fracture surfaces of compact tensile samples of a weldment in an HSLA quenched and tempered steel using radiography, optical and electron optical techniques. These fish eyes were examined in detail.

The presence of the fish eyes and three fracture regions, separated by curved lines, are evident in Figure 1. The surface at the point of initiation of the fracture through the fish eyes is characterised by a smooth shiny surface (Figures 2 and 3). During solidification the formation of a pore with a smooth surface is the result of gas entrainment and for the surface to be shiny the gas must be non-oxidising. This would suggest that hydrogen is the most likely gas in this instance. As the crack propagates from the point of initiation the fracture surface has a directional appearance (Figure 4) quite different to that of the material surrounding the fish eye. All of the fish eyes examined in the present study contained gas pores. The appearance of the fractures within the fish eyes indicates that fracture had initiated at the gas pores.

The X-ray line scans acquired using the EPMA show that the segregation of all elements ahead of the crack tip is coincident at approximately 50µm intervals perpendicular to the crack growth direction. The alloying elements have segregated in the ratio of 1.4:1 as stated previously which is in agreement with that previously reported for intercellular-dendritic segregation in a low alloy steel weld (5). This segregation was not detected when the sample was etched in Nital suggesting that it is intercellular-dendritic segregation resulting from the solidification of the weld metal to delta ferrite. The distance between the cracks in the fish eye is also approximately 50µm when measured in a direction perpendicular to the crack growth direction. This is within the predicted size range for the cell diameter in steel arc welds.

The appearance of the fracture suggests that it is of a brittle nature and that the fracture path has followed the intercellular-dendritic segregation. The microstructure in these intercellular-dendritic regions is much more likely to contain bainite/martensite due to the higher alloy content and is therefore more susceptible to cracking.

Banding It is not unusual to find macro-segregation or banding in welds in multi-pass welds and several mechanisms have been proposed for their formation (12). The common feature of these mechanisms is that banding is a consequence of a variation in the rate of solidification resulting from changes in either heat input or heat extraction during welding. However there is little information available on the composition of these bands in low alloy steel welds. As is the case with microsegregation, it could be expected that all elements would segregate to the same degree in these macro-segregated areas. The degree of segregation would be dependent upon the partitioning characteristics of the system (4). By the same argument used above for microsegregation, it would not be unexpected to find cracking associated with these regions due to their higher alloy content and therefore increased susceptibility to cracking. However, what is unusual about the present example is that X-ray line scans across the band using the EPMA (Figure 10) indicate that only

manganese has segregated in the band. The profile of the concentration of the manganese within the band is as expected for an increase in growth rate of the solid from the weld pool of a pure ternary system (12).

Ongoing research will endeavour to determine the mechanism for the current result and whether these bands can be related to the lines seen on the fracture surface separating the three fracture zones (Figure 1).

Summary and Conclusions

Evidence is presented to suggest that both micro-segregation and macro-segregation occur during the solidification of low alloy steel weldments. Micro-segregation appears to be associated with the cracking in fisheyes. A small gas pore, probably hydrogen, was found at the fracture initiation sites of each fish eye.

Macro-segregated bands containing only increased levels of manganese were found. These bands were probably the result of variations in welding parameters resulting from an increase in the solidification rate. Some of these bands contained cracks.

Acknowledgements

The authors wish to acknowledge the support of the Australian Defence Science and Technology Organisation, Maritime Platforms Division.

References

1. N. Yurioka and H. Suzuki, *Int. Mater. Rev.*, 35, 217-249 (1990)
2. J.L. Davidson, S.P. Lynch and A. Madumdar, *The Relationship Between Hydrogen-Induced Cracking Resistance, Microstructure and Toughness in High Strength Weld Metal*, in *Hydrogen Management in Steel Weldments*, J.L. Davidson and D.L. Olson (Eds.), Joint Defence Science and Technology Organisation/Welding Technology Institute of Australia Seminar, Melbourne, Australia, 21-34 (1996)
3. W.F. Savage, *Welding in the World*, 18, 89-114 (1980)
4. G.J. Davies and J.G. Garland, *Int. Metall. Rev.*, 20, 83-106 (1975)
5. G.L.F. Powell and P.G. Lloyd, *Prakt. Metallogr.*, 32, 25-31 (1995)
6. G.L.F. Powell and G. Herfurth, *Metall. Mater. Trans.*, 29A, 2775-2784 (1998)
7. A.A.B. Sugden and H.K.D.H. Bhadeshia, *Metall. Trans.*, 19A, 669-674 (1988)
8. F.S. LePera, *J. Met.*, 32, 38-39 (1980)

9. *Metals Handbook*, 9th Ed., ASM, Metals Park, OH, Vol.6, 7 (1983)
10. D. Seferian, *The Metallurgy of Welding*, p.150, Chapman and Hall, London (1962)
11. B.F. Dixon and J.S. Taylor, *Control of Hydrogen Cracking in Collins Class Submarine Welds*, in *Hydrogen Management in Steel Weldments*, J.L. Davidson and D.L. Olson (Eds.), Joint Defence Science and Technology Organisation/Welding Technology Institute of Australia Seminar, Melbourne, Australia, 125-144 (1996)
12. S.A. David and J.M. Vitek, *Int.Mater. Rev.*, 34, 213-246 (1989)